ELSEVIER

Journal of Organometallic Chemistry 574 (1999) 142–147

Journal of Organometallic Chemistry

# Synthesis and structure of 1,3-dienolate ($CH_2C(O)CH{=}CH_2$) complex of dipalladium(I) moiety: contribution of $\pi$-olefin co-ordination of enolate to transition metal☆

Tetsuro Murahashi, Hideo Kurosawa *

*Department of Applied Chemistry, Faculty of Engineering, Osaka University, Suita, Osaka 565-0871, Japan*

Received 1 July 1998; received in revised form 3 August 1998

**Abstract**

1,3-Dienolate dipalladium(I) complex [{$\mu$-$CH_2C(O)CH{=}CH_2$}$Pd_2(PPh_3)_2(\mu$-Cl)] (**2**) is prepared and characterized. Complex **2** is easily protonated to yield 2-hydroxy-1,3-butadiene dipalladium(I) complex [{$(\mu$-$\eta^2$:$\eta^2$-$CH_2{=}C(OH)CH{=}CH_2$}$Pd_2(PPh_3)_2(\mu$-Cl)][$BF_4$] (**3**). On the basis of the comparative analyses on IR and NMR spectra and X-ray structure analysis, the co-ordination mode of 1,3-dienolate on Pd–Pd is revealed to involve the resonance between C-bound and $\pi$-olefin-bound enolate structures.


*Keywords:* Enolate; Palladium; Dinuclear

## 1. Introduction

Transition metal enolate complexes have been proposed as the important intermediates in several organic transformations [1]. Previously, three types of enolate complexes, C-bound form (A), O-bound form (B), and oxallyl form (C) (Scheme 1) were reported with a wide variety of early and late transition metals [1]. These exhibited different reactivities depending on the co-ordination mode of the enolate moiety [2]. In palladium enolate chemistry, all of the above three types of complexes have been isolated and characterized [3,4], or proposed as the intermediate of several catalytic processes [5]. The authors thought another possible co-ordination mode, D, is of great interest, since this is expected to bring a new entry to enolate transformation involving the transition metal center, e.g. insertion reaction of enolate into a metal–carbon bond. However, to the best of the authors knowledge, an enolate complex of type D is entirely unprecedented. In view of the fact that mononuclear metal systems generally favor the types A–C, attention has turned to a dinuclear system, in which the adjacent metal is expected to assist generating a new bonding mode of the bridging ligands.

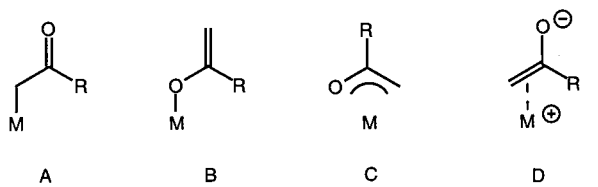


Scheme 1.

Also noticed was a prominent feature in the type D enolate complex, namely the zwitterionic structure. The zwitterionic structure in organometallic complexes has been recognized as a key factor in changing the electron density on the metal center, or bringing about the higher stability of the complex compared with the

☆ Dedicated to the late Professor Rokuro Okawara in memory of his lifetime guidance and encouragement in our research of organometallic chemistry.

* Corresponding author. Tel.: +81-6-879-7392; Fax: +81-6-879-7394.

0022-328X/99/$ - see front matter 
PII: S0022-328X(98)00934-6

corresponding non-ionic complexes [6]. However, the zwitterionic aggregate through $\pi$-bonding, which is found in the structure of type D, has rarely been observed in organometallic compounds. Recently, it has been reported that the zwitterionic structure in the complex **1a** is more stable than the alternative neutral structure **1b** [7]. While the sterically unfavorable *cis* arrangement of two phosphine ligands at the mononuclear Pd center would partially contribute to destabilization of **1b**, the result implies that the zwitterionic structure is a reality in the $\eta^2$:$\eta^2$-diene dipalladium system. Thus, the authors examined if the 1,3-dienolate anion can analogously co-ordinate on the $Pd_2(\mu\text{-Cl})(PPh_3)_2$ cation in a zwitterionic manner.

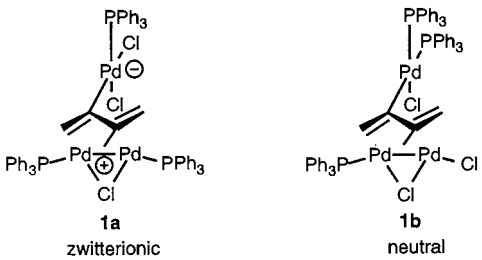


## 2. Results and discussion

$\mu$-$\eta^2$:$\eta^2$-Dienolate dipalladium(I) complex **2** was prepared by the reaction of an equimolar mixture of Pd(II) complex $[Pd(PPh_3)_2Cl]_2[PF_6]_2$ and Pd(0) complex $Pd_2(dba)_3$ with 2-trimethylsiloxy-1,3-butadiene in the presence of base ($Et_3N$) in 35% isolated yield (Eq. (1)). The dienolate dipalladium complex **2** was also prepared by 1,3-diene ligand exchange reaction of $[(\mu\text{-1,3-butadiene})Pd_2(PPh_3)_2(\mu\text{-Cl})][PF_6]$ [8] followed by desilylation of 2-trimethylsiloxy-1,3-butadiene co-ordinated on the Pd–Pd bond in the presence of $Et_3N$ in 67% isolated yield (Eq. (2)).

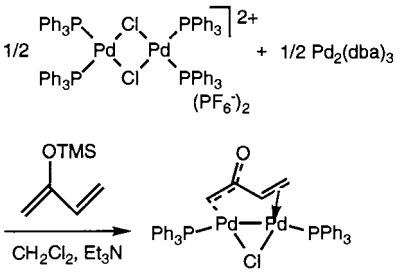


(1)

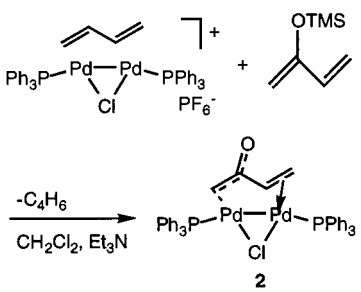


(2)

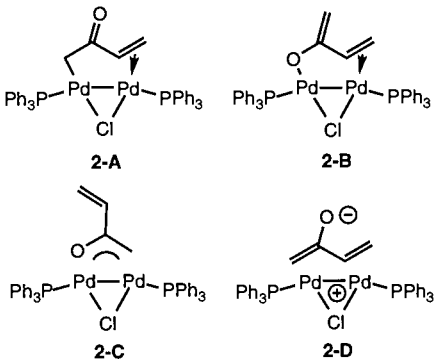


Scheme 2.

When the 1,3-dienolate complex, **2**, was treated with one equivalent of $HBF_4$, the protonated product **3** was generated almost quantitatively (Eq. (3)). The 2-hydroxydiene complex **3** was easily deprotonated to regenerate **2** by treating with base, such as $Et_3N$ in $CDCl_3$.

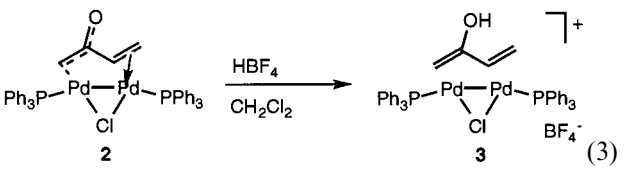


(3)

As to the 1,3-dienolate co-ordination mode on the Pd–Pd, there are several possible structures; C-bound ($\mu$-$\eta^1$:$\eta^2$) (**2-A**), O-bound ($\mu$-$\eta^1$:$\eta^2$) (**2-B**), $\mu$-oxallyl ($\mu$-$\eta^3$) (**2-C**), and $\pi$-olefin-bound ($\mu$-$\eta^2$:$\eta^2$) (**2-D**) as shown in Scheme 2.

IR and NMR spectroscopic data of **2**, **3** and related enolate complexes are listed in Table 1. **2-B** and **2-C** can be ruled out, since no free methylene or vinyl proton resonances were detected (see Section 4). IR spectra of **2** showed the C=O stretching absorbance at 1596 $cm^{-1}$, which is approximately 20–40 $cm^{-1}$ lower in energy than those of the previously reported Pd(II) mononuclear enolate complexes [3]. These obviously indicate that the formal C–O bond order in **2** is reduced from those in the typical C-bound Pd enolate complexes. $^{13}$C-NMR spectra of **2** showed a strongly shielded carbonyl carbon resonance at $\delta$ 168.9 compared with those of Pd(II) complexes **4**–**8**. As expected, the carbonyl carbon resonance moved to the still higher field (140.1 ppm in **3**) upon protonation of **2**. Since the chemical shifts of the enolate carbons (especially $C_\alpha$) might depend on the electronic effect of the directly attaching transition metals, little might be deduced from these shifts. However, the values of $J_{CH}$ and $J_{HH}$ for the $\alpha$-$CH_2$ group appear more informative. Comparison of these coupling constants between **2** and **4** or **6** suggests that the $\alpha$-carbon of **2** bears a greater $sp^2$ character than that of **4** and **6**. Again, the correspond-

Table 1
Relevant spectroscopic data for palladium and nickel enolate complexes

| | IR | NMR | | | | | Reference |
|---|---|---|---|---|---|---|---|
| | $\nu$(C=O) ($cm^{-1}$) | $J_{HaHb}$ | $\delta_{(C-O)}$ | $\delta_{(C\alpha)}$ ($J_{CH}$) | $\delta_{(C\gamma)}$ ($J_{CH}$) | $\delta_{(C\delta)}$ ($J_{CH}$) | |
| **2** | 1596 | 5.10 | 168.9 | 52.0 (147.9) | 74.4 (154.6) | 43.9 (157.3) | This work |
| **3** | – | 1.95 | 140.1 | 52.7 (159.6) | 73.3 (165.5) | 44.1 (160.2) | This work |
| **4** | 1624 | – | 204.5 | 30.5 (135.0) | — | — | [3a] |
| **5** | 1670 | – | 220.1 | 31.3 | — | — | [3c] |
| **6** | 1643 | 10.60 | 207.5 | 40.5 | — | — | [3a] |
| **7** | 1634 | – | 220.8 | 9.85 | — | — | [3b] |
| **8** | 1682 | – | 181.0 | 0.8 | — | — | [3b] |
| **9** | 1675 | – | 182.8 | 0.8 | — | — | [3b] |
| **10** | 1682 | – | 181.0 | 6.48 | — | — | [3b] |

ing carbon atom in **3** has a still greater $sp^2$ character, as judged from larger $J_{CH}$ and smaller $J_{HH}$. The observed carbonyl stretching absorbance, chemical shifts for carbonyl carbon, geminal $J_{HH}$ on $C_\alpha$, C–H coupling for $C_\alpha$–H of **2** are all in good agreement with the resonance form between **2-A** and **2-D**. Akita et al. previously reported a similar partial contribution of $\pi$-bound structure **11-D** in a metalloenolate complex ($\mu$-ketene complex) on the basis of the lower shifted carbonyl absorbance than the related acyl–Fe complex [9].

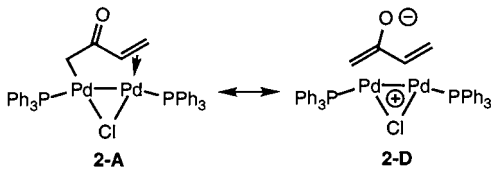


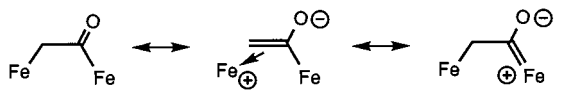


For determining the solid state structure of **2**, X-ray crystal structure analysis was undertaken. The ORTEP diagram is shown in Fig. 1. The Pd–Pd bond length is 2.6968(6) Å, which is in the range of normal Pd–Pd bond lengths [10]. Unfortunately, the inner carbon and oxygen atoms of the bridging dienolate moiety are disordered to make a precise discussion about the structural parameters of the dienolate ligand difficult (relative occupancy for C2–C3–O1/C2′–C3′–O1′ was set as 60/40). However, as predicted by the spectroscopic analyses, the co-ordination mode of dienolate in **2** is revealed to be **2-A** or **2-D** but neither **2-B** nor **2-C**. The mean dihedral angle between dienolate plane (C2–C3–C4/C1–C2′–C3′) and dipalladium core plane (Pd1–Pd2–Cl1) is 65° [11], which was smaller than that of $\pi$-bound $\mu$-butadiene dipalladium complex [($\mu$-$\eta^2$:$\eta^2$-$C_4H_6$)$Pd_2$($PPh_3$)Br($\mu$-Br)] (92°) [8]. This indicates that the dienolate co-ordination geometry in **2** is not consistent with the full structural contribution of **2-D**. However, the bond distance between the carbonyl carbon and the near Pd atom (Pd1–C2′, Pd2–C3, 2.46(2) Å) is shorter than those of the structurally determined C-bound enolate complexes (e.g. 2.685 Å for **4** and 2.818 Å for **6**) [3a], again indicating partial contribution of $\pi$-enolate form (**2-D**). It is noteworthy that the crystal structure suggests the presence of a relatively short O···H–C contact between the oxygen of the dienolate and the hydrogen of the chloroform incorporated during crystallization. The observed O···C distance (3.00(1) Å for O1–C43 and O1′–C43) is shorter than the mean distances of O···C involved in O···H–C hydrogen bonds found from the Cambridge Database search

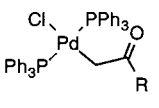


**4** (R = Ph)
**5** (R = $^t$Bu)

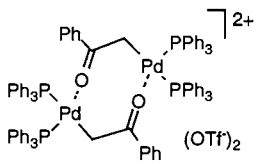


**6**

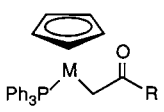


**7** (M = Pd, R = $^t$Bu)
**8** (M = Pd, R = O$^t$Bu)
**9** (M = Ni, R = $^t$Bu)
**10** (M = Ni, R = CH=$CH_2$)

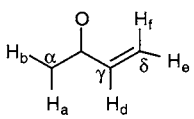


Numbering scheme

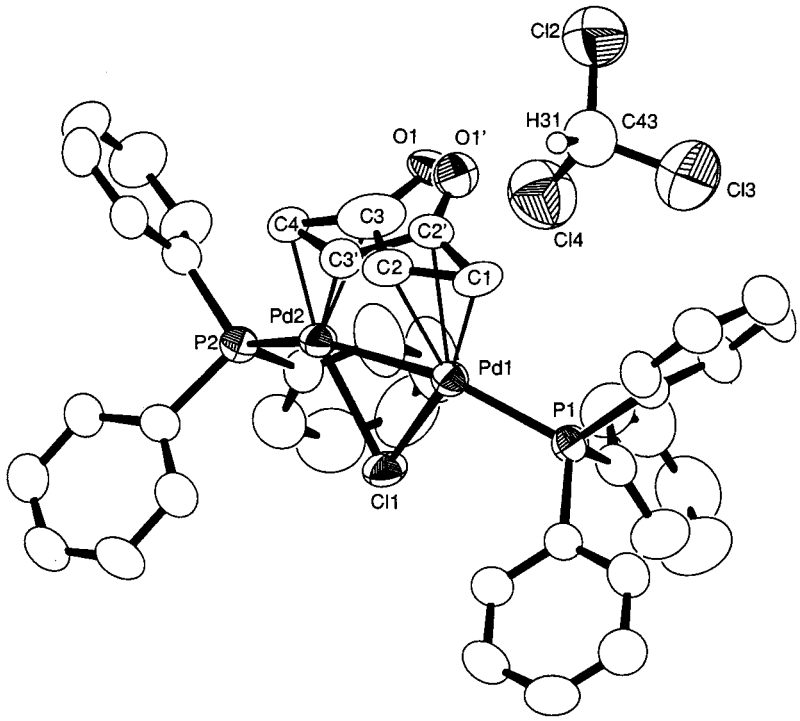


Fig. 1. ORTEP drawing of **2**. Selected bond distances (Å) and angles (°): Pd1–Pd2, 2.6968(6); Pd1–P1, 2.258(2); Pd2–P2, 2.262(2); Pd1–Cl1, 2.379(1); Pd2–Cl1, 2.392(1); Pd1–Pd2–Cl1, 55.36(4); Pd1–Pd2–P2, 154.15(4); Pd1–Cl1–Pd2, 68.64(4); Pd2–Pd1–P1, 153.18(4).

(3.32 Å) [12]. This hydrogen bonding might be derived from the localization of partial anionic charge on the enolate oxygen atom associated with the structure **2-D**.

## 3. Conclusion

The authors propose in this work that when 1,3-dienolate is co-ordinated on the Pd–Pd bond, the co-ordination mode is represented by a resonance form between C-bound enolate (**2-A**) and $\pi$-olefin-bound enolate (**2-D**). The spectroscopic and X-ray crystal structural analyses of **2** were in agreement with this resonance structure. The new co-ordination geometry of enolate to transition metal (**2-D**) has a possibility to bring a new entry of organometallic transformation of enolate such as migratory insertion.

## 4. Experimental

Solvents were generally freshly distilled before use: dichloromethane from calcium hydride; *n*-hexane from benzophenone ketyl. Triethylamine was distilled from calcium hydride. 2-Trimethylsiloxy-1,3-butadiene and $HBF_4 \cdot Et_2O$ (85%) were purchased and used without further purification. $^1$H-, $^{13}$C- and $^{31}$P-NMR spectra were recorded using a JEOL GSX-270 (270 MHz) or JEOL JSX-400 (400 MHz) spectrometer. IR spectra were recorded using JASCO FT/IR-3. All manipulations were performed under argon atmosphere using Shlenck techniques.

### 4.1. Synthesis of [($\mu$-1,3-butadiene)$Pd_2(PPh_3)_2$ ($\mu$-Cl)][$PF_6$]

$[Pd(PPh_3)_2Cl]_2[PF_6]_2$ was generated from $Pd(PPh_3)_2Cl_2$ and $AgPF_6$ in $CH_2Cl_2$, and used as a mixture with two equivalents of AgC1 because of its poor solubility. 1,3-Butadiene gas was bubbled through the suspension mixture of $[Pd(PPh_3)_2Cl]_2[PF_6]_2$ and 2AgCl (134.2 mg, excess) and $Pd_2(dba)_3$ (57.0 mg, 0.0551 mmol) in $CH_2Cl_2$ at r.t.. After bubbling for 0.5 h, the reaction mixture was filtered, and the volatile materials were removed in vacuo. The residues were washed with *n*-hexane and dried under vacuum. Recrystallization from $CH_2Cl_2/Et_2O$ gave vivid-orange crystals (51.1 mg, 46% yield). $^1$H-NMR ($CDCl_3$), $\delta$ 7.7–7.5 (30H, m, Ph), 3.61 (2H, br d), 3.46 (2H, br m), 2.98 (2H, br d). $^{13}$C-NMR ($CDCl_3$), $\delta$ 134–129 (Ph), 93.41, 59.42. $^{31}$P-NMR ($CDCl_3$), $\delta$ −111.33 (s). Anal. Calc. (found) for $C_{40}H_{36}Pd_2ClP_3F_6$: C, 49.43 (49.34); 3.73 (3.80).

### 4.2. Synthesis of ($\mu$-1,3-dienolate)$Pd_2(PPh_3)_2(\mu$-Cl) (**2**)

To a $CH_2Cl_2$ solution of [($\mu$-1,3-butadiene)$Pd_2(PPh_3)_2$($\mu$-Cl)][$PF_6$] (1.00 g, 1.03 mmol), 2-trimethylsiloxy-1,3-butadiene (272 μl, 1.54 mmol) and $Et_3N$ (170 μ1, 1.22 mmol) were added and the reaction mixture was stirred for 1.5 h at r.t. The yellow solution was filtered

and the filtrate was evaporated. The residue was washed with *n*-hexane and resolved in $CH_2Cl_2$ and the solution passed through silica gel column (Wakogel C-200, 50 g) to give a yellow solution. Recrystallization from $CH_2Cl_2$/*n*-hexane gave yellow crystals of **2** (577 mg, 67% yield). $^1$H-NMR ($CD_2Cl_2$), $\delta$ 7.7–7.4 (30H, m, Ph), 3.31 (1H, m, $H_d$), 3.04 (1H, br d, $H_f$), 2.55 (2H, br dd, $H_b$, $H_e$), 2.45 (1H, m, $H_a$) (for numbering, see Table 1). $^{31}$P-NMR ($CD_2Cl_2$), $\delta$ −106.40 (d, $J=73$ Hz), −119.52 (d, $J=73$ Hz). $^{13}$C-NMR ($CD_2Cl_2$), $\delta$ 168.9 (C=O), 134–129 (Ph), 74.36 ($C_\gamma$), 52.01 ($C_\alpha$), 43.92 ($C_\delta$). Anal. Calc. (found) for $C_{40}H_{35}Pd_2ClP_2O$: C, 57.06 (57.02); 4.19 (4.08).

Alternatively, to a suspension mixture of $[Pd(PPh_3)_2Cl]_2[PF_6]_2$ and two equivalents of AgCl (277 mg, 0.145 mmol), $Pd_2(dba)_3$ (100 mg, 0.0966 mmol) was added. Subsequently, 2-trimethylsiloxy-1,3-butadiene (51.2 μl, 0.290 mmol) and $Et_3N$ (27.0 μl, 0.193 mmol) were added at r.t. After 7 h, the red solution was passed through silica gel column (Wakogel C-200) to give a yellow solution. Crystallization gave yellow crystals of **2** (57.7 mg, 35% yield).

### 4.3. Synthesis of [(μ-η²:η²-2-hydroxy-1,3-dienolate) $Pd_2(PPh_3)_2$(μ-Cl)][$BF_4$] (3)

To a $CH_2Cl_2$ solution of **2** (65.6 mg, 0.0779 mmol), $HBF_4{\cdot}Et_2O$ (13.5 μl, 0.0779 mmol) was added and the reaction mixture was stirred for 30 min at r.t. The yellow solution was filtered off, then evaporated and dried in vacuo. Reprecipitation from $CH_2Cl_2$/*n*-hexane solution gave orange–yellow powder of **3** (43.8 mg, 60% yield). $^1$H-NMR ($CD_2Cl_2$), $\delta$ 7.7–7.4 (30H, m, Ph), 3.66 (1H, br dd, $H_b$), 3.09 (1H, ddd, $H_f$), 2.93 (1H, br ddd, $H_e$), 2.65 (1H, dd, $H_a$), 2.62 (1H, m, $H_d$). $^{31}$P-NMR ($CD_2Cl_2$), $\delta$ −109.60 (d, $J=75$ Hz), −112.16 (d, $J=75$ Hz). $^{13}$C-NMR ($CD_2Cl_2$), $\delta$ 140.1 (C–O), 134–129 (Ph), 74.3 ($C_\gamma$), 52.7 ($C_\alpha$), 44.1 ($C_\delta$). Anal. Calc. (found) for $C_{40}H_{35}Pd_2ClP_2OBF_4$: C, 51.67 (51.42); 3.90 (4.14).

### 4.4. X-ray crystallographic analysis of 2

A yellow prismatic crystal of **2** having approximate dimensions of $0.30\times0.30\times0.40$ mm$^3$ was mounted into a glass capillary. All measurements were made on a Rigaku AFC5R diffractometer with graphite monochromated Mo–$K_\alpha$ radiation. Cell constants and an orientation matrix for data collection corresponded to a primitive triclinic cell with dimensions listed below. Based on a statistical analysis of intensity distribution, and the successful solution and refinement of the structure of 298 K to a maximum $2\theta$ value of 55.1°, the space group was determined to be $P2_1/c$ (No. 14). A

Table 2
Atomic co-ordinates for [(μ-$CH_2C(O)CHCH_2$)$Pd_2(PPh_3)_2$(μ-Cl)]·$CHCl_3$

| Atom | *x* | *y* | *z* | Atom | *x* | *y* | *z* |
|---|---|---|---|---|---|---|---|
| Pd(1) | 0.13460(3) | 0.11221(3) | 0.07268(2) | C(16) | 0.3572(5) | −0.2049(4) | 0.1554(4) |
| Pd(2) | 0.17087(3) | 0.05171(3) | 0.04803(2) | C(17) | 0.1390(4) | 0.3126(3) | 0.1561(3) |
| Cl(1) | 0.2188(1) | −0.06724(9) | −0.01293(8) | C(18) | 0.0433(4) | −0.3286(4) | 0.1481(3) |
| Cl(2) | 0.6562(2) | −0.0048(2) | 0.5654(2) | C(19) | 0.0160(4) | −0.3702(4) | 0.2035(4) |
| Cl(3) | 0.6491(2) | 0.1586(2) | 0.6291(2) | C(20) | 0.0824(5) | 0.3962(4) | 0.2680(4) |
| Cl(4) | 0.6066(2) | 0.0114(2) | 0.7028(1) | C(21) | 0.1768(5) | 0.3788(5) | 0.2769(3) |
| P(1) | 0.1712(l) | −0.25211(9) | 0.08333(8) | C(22) | 0.2060(4) | −0.3385(4) | 0.2219(3) |
| P(2) | 0.2605(1) | 0.15874(9) | 0.02283(8) | C(23) | 0.2352(4) | 0.1841(4) | −0.0775(3) |
| O(1) | 0.1607 | 0.0286 | 0.2308 | C(24) | 0.2440(4) | 0.2652(4) | −0.1042(3) |
| O(1′) | 0.1392 | −0.0063 | 0.2329 | C(25) | 0.2265(5) | 0.2791(4) | −0.1805(4) |
| C(1) | 0.0570(4) | −0.1129(4) | 0.1501(3) | C(26) | 0.2021(5) | 0.2138(5) | −0.2302(3) |
| C(2) | 0.0470(10) | −0.021(1) | 0.116(1) | C(27) | 0.1910(5) | 0.1341(4) | −0.2061(3) |
| C(2′) | 0.090(2) | −0.030(1) | 0.170(1) | C(28) | 0.2073(5) | 0.1193(4) | −0.1295(3) |
| C(3) | 0.108(1) | 0.044(1) | 0.158(1) | C(29) | 0.2625(4) | 0.2633(3) | 0.0657(3) |
| C(3′) | 0.058(2) | 0.033(2) | 0.104(1) | C(30) | 0.1758(4) | 0.3044(4) | 0.0575(3) |
| C(4) | 0.1024(5) | 0.1192(4) | 0.1126(4) | C(31) | 0.1736(5) | 0.3852(4) | 0.0857(4) |
| C(5) | 0.1246(4) | −0.3148(3) | −0.0024(3) | C(32) | 0.2567(7) | 0.4253(4) | 0.1226(4) |
| C(6) | 0.1063(4) | −0.2761(4) | −0.0719(3) | C(33) | 0.3428(6) | 0.3859(5) | 0.1317(4) |
| C(7) | 0.0762(5) | 0.3220(4) | −0.1383(3) | C(34) | 0.3458(5) | 0.3049(4) | 0.1036(4) |
| C(8) | 0.0654(5) | −0.4082(4) | −0.1355(4) | C(35) | 0.5403(6) | 0.1152(6) | 0.0349(6) |
| C(9) | 0.0826(5) | −0.4477(4) | −0.0675(4) | C(36) | 0.4471(5) | 0.1431(5) | 0.0115(4) |
| C(10) | 0.1120(4) | −0.4010(4) | −0.0008(3) | C(37) | 0.3852(4) | 0.1250(4) | 0.0516(3) |
| C(11) | 0.3009(4) | −0.2628(4) | 0.1081(3) | C(38) | 0.4173(5) | 0.0781(5) | 0.1149(5) |
| C(12) | 0.3441(5) | −0.3281(5) | 0.0814(4) | C(39) | 0.5121(7) | 0.0490(7) | 0.1392(6) |
| C(13) | 0.4417(6) | −0.3349(6) | 0.1036(5) | C(40) | 0.5704(6) | 0.0661(7) | 0.0974(7) |
| C(14) | 0.4975(5) | −0.2778(7) | 0.1514(5) | C(43) | 0.6771(5) | 0.0529(5) | 0.6491(4) |
| C(15) | 0.4566(6) | −0.2124(6) | 0.1783(5) | | | | |

total of 5855 reflections was collected ($I > 3\sigma(I)$). The linear absorption coefficient, $\mu$, for Mo–$K_\alpha$ radiation was 12.66 $cm^{-1}$. The data were corrected for Lorenz and polarization effects.

Crystal data for 2·$CHCl_3$: $Pd_2C_{41}H_{36}Cl_4P_2O$, $M = 961.29$, monoclinic, space group $P2_1/c$ (No. 14), $a = 14.581(3)$, $b = 15.724(3)$, $c = 18.458(3)$ Å, $\beta = 107.33(1)°$, $U = 4039(1)$ $Å^3$, $Z = 2$, $D_{calc.} = 1.581$ g $cm^{-3}$, $F(000) = 1920$, $\mu$(Mo–$K_\alpha$) = 12.66 $cm^{-1}$, 652 variables refined with 5855 reflections collected with $I > 3\sigma(I)$ to $R = 0.050$, $R_w = 0.039$. Atomic co-ordinates are listed in Table 2.

## Acknowledgements

Partial support of this work through Grant-in-Aid for Scientific Research, Ministry of Education, Science and Culture, and CREST of Japan Science and Technology Corporation is gratefully acknowledged. T.M. acknowledges the JSPS research fellowships for young scientists. Thanks are also due to the Analytical Center, Faculty of Engineering, Osaka University for the use of NMR facilities.

## References

[1] C.H. Heathcock, in: B.M. Trost (Ed.), Comprehensive Organic Synthesis, vol. 2, Pergamon, New York, 1991, Chaps. 1.5 and 1.6.

[2] J.G. Stack, J.J. Doney, R.G. Bergman, C.H. Heathcock, Organometallics 9 (1990) 453.

[3] Type A (a) P. Veya, C. Floriani, A. Chiesi-Villa, C. Rizzori, Organometallics 12 (1993) 4899. (b) E.R. Burkhardt, R.G. Bergman, C.H. Heathcock, Organometallics 9 (1990) 30. (c) R.A. Wanat, D.B. Collum, Organometallics 5 (1986) 120. Type B (d) S-E. Bouaoud, P. Braustein, D. Gradjean, D. Matt, D. Nobel, J. Chem. Soc. Chem. Commun. (1987) 488. (e) Y. Ito, M. Nakatsuka, N. Kise, T. Saegusa, Tetrahedron Lett. 21 (1980) 2873. Type C (f) N. Yoshimura, S.-I. Murahashi, I. Moritani, J. Organomet. Chem. 52 (1973) C58.

[4] All three co-ordination modes were also found in the $\beta$-dicarbonyl anion (RC(O)CHC(O)R′)–palladium complexes. S. Kawaguchi, in: H. Yaozeng, A. Yamamoto, B.-K. Teo (Eds.), New Frontiers in Organometallic and Inorganic Chemistry, Science Press, Beijing, 1984, p. 101.

[5] (a) J. Ahman, J.P. Wolfe, M.V. Troutman, M. Palucki, S.L. Buchwald, J. Am. Chem. Soc. 120 (1998) 1918. (b) M. Palucki, S.L. Buchwald, J. Am. Chem. Soc. 119 (1997) 11108. (c) B. Hamann, J.F. Hartwig, J. Am. Chem. Soc. 119 (1997) 12382. (d) H. Muratake, A. Hayakawa, M. Natsume, Tetrahedron Lett. 38 (1997) 7577. (e) H. Muratake, M. Natsume, Tetrahedron Lett. 38 (1997) 7581. (f) A. Satoh, Y. Kawamura, M. Miura, M. Nomura, Angew. Chem. Int. Ed. Engl. 36 (1997) 1740. (g) M. Sodeoka, K. Ohrai, M. Shibasaki, J. Org. Chem. 60 (1995) 2648. (h) J. Nokami, T. Mandai, H. Watanabe, H. Ohyama, J. Tsuji, J. Am. Chem. Soc. 111 (1989) 4126. (i) J. Tsuji, I. Minami, Acc. Chem. Res. 20 (1987) 140. (j) Y. Ito, H. Aoyama, T. Saegusa, J. Am. Chem. Soc. 102 (1980) 4519. (k) Y. Ito, H. Aoyama, T. Hirao, A. Mochizuki, T. Saegusa, J. Am. Chem. Soc. 101 (1979) 496. (l) Y. Ito, T. Hirao, T. Saegusa, J. Org. Chem. 43 (1978) 1011.

[6] For example, H. van der Heijden, B. Hessen, A.G. Orpen, J. Am. Chem. Soc. 120 (1998) 1112, and references therein.

[7] T. Murahashi, H. Kurosawa, N. Kanehisa, Y. Kai, J. Organomet. Chem. 530 (1997) 187.

[8] T. Murahashi, N. Kanehisa, Y. Kai, T. Otani, H. Kurosawa, J. Chem. Soc. Chem. Commun. (1996) 825.

[9] M. Akita, A. Kondoh, T. Kawahara, T. Takagi, Y. Moro-oka, Organometallics 7 (1988) 366.

[10] T. Murahashi, T. Otani, E. Mochizuki, Y. Kai, H. Kurosawa, S. Sakaki, J. Am. Chem. Soc. 120 (1998) 4536.

[11] This value of dihedral angle reflects the degree of displacement of carbonyl carbon (C3/C2′) from the plane formed by the other dienolate carbons, while the mean dihedral angle between C1–C2–C4/C1–C3′–C4 and Pd1–Pd2–Cl1 core is 95°, near to 90°.

[12] (a) G.R. Desiraju, J. Chem. Soc. Chem. Commun. (1989) 179. (b) G.R. Desiraju, Acc. Chem. Res. 29 (1996) 441.